Kinetics of initial biofilm formation within a turbulent flow system

Authors: James D. Bryers and William G. Characklis

Bryers, J.D. and W.G. Characklis, "Kinetics of Initial Biofilm Formation Within a Turbulent Flow system," in E.F.C. Somerscales and J.G. Knudsen (eds.), Fouling of Heat Transfer Equipment, Hemisphere Publishing Corp., Washington, DC, 1981, pp. 313-333.

KINETICS OF INITIAL BIOFILM FORMATION WITHIN A TURBULENT FLOW SYSTEM

JAMES D. BRYERS
University of Calgary, Calgary, Alberta, Canada

WILLIAM G. CHARACKLIS
Montana State University, Bozeman, Montana, U.S.A.

(both formerly with Rice University, Houston, Texas, U.S.A.)

ABSTRACT

A kinetic expression is presented which describes biofouling film development from clean surface conditions to the onset of fluid frictional resistance increase. Biofouling experiments were conducted in a C.S.T.R. with internal recycle; a system which provided control of biological activity in the bulk fluid while simulating turbulent flow conditions. The effect of three system parameters--dispersed biomass concentration, Reynolds Number, and dispersed biomass growth rate--on the rate of initial biofilm formation is presented. Primary biofilm accumulation is described using a first order rate expression with the resultant first order rate constant a linear function of the considered parameters.

1. INTRODUCTION

Biofouling film development in a turbulent flow system progresses sigmoidally as illustrated in Fig. 1. Three phases are evident:

1. Initial Biofilm Formation
2. An Exponential Accumulation
3. Steady State or Plateau Phase

The induction or initial formation phase terminates when both frictional and heat transfer resistances begin to increase, as shown in Fig. 1. The effects of biofilm on both frictional and heat transfer resistance become economically important in the latter two stages of development. A majority of research has focused on these two biofilm development phases [1,2].

However, research indicates that the physical, chemical, and biological properties of biofilms may be determined within the initial formation stage [3, 4,5,6]. In ocean thermal energy conversion (OTEC) systems, thermal efficiency criteria dictate maximum tolerable biofilm amounts that are characteristic of the initial formation period [7,8]. Control of biofilms in the past has been by the unsystematic application of chlorine; a procedure which has been restricted by new effluent chlorine standards. Stoichiometry suggests the use of chemical controls is more efficient in the early stages of biofouling. All these applications justify research into the kinetics of initial biofilm formation. Previous research regarding initial biofilm formation has generally ignored the

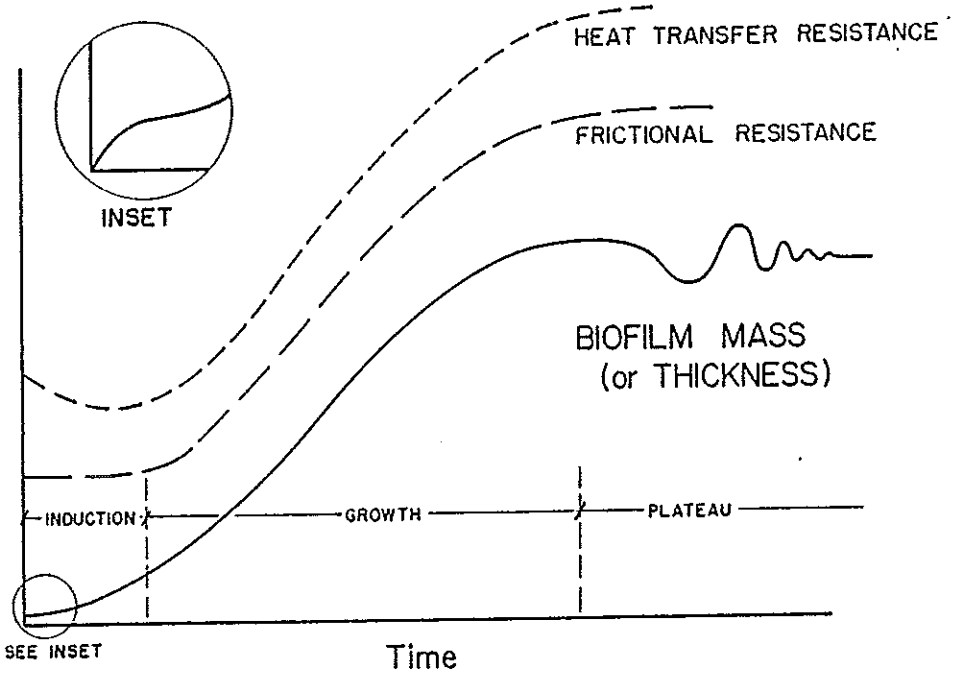

Fig. 1. Progression of biofouling

effects of parameters of engineering concern. This work is an attempt to define the kinetic aspects of initial biofilm accumulation within a turbulent flow system.

2. PROCESS CONTRIBUTING TO BIOFILM DEVELOPMENT

Microbial fouling is the net result of physical transport and biological growth rate processes, as shown in Fig. 2. Evidence suggests the following processes contribute to overall biofouling accumulation:

1. Organic adsorption at the wetted surface--Adsorption of an organic layer occurs within minutes of exposure. Investigations show that materials with diverse surface properties (e.g., wettability, surface tension, electrophoretic mobility) are rapidly conditioned by adsorbing organics once exposed to natural waters with low organic concentrations [9,10,11,12,13,14].

2. Transport of microbial particles to the surface--Within a turbulent flow regime, particles suspended within the fluid are transported to the surface by only two mechanisms: molecular diffusion and turbulent eddy transport [15,16]. Chemotaxis does not appear to be a significant mechanism for particle migration to a surface where fluid shear exists [17].

3. Microorganism attachment to the surface--Research suggests the existence of a two-stage attachment process: reversible adhesion followed by an irreversible attachment. Many of the microbial cell attachment studies were conducted at very low fluid shear rates or under quiescent conditions [18,19,20,21]. Rates of accumulation from these studies are very likely mass transfer-limited and not necessarily applicable to condenser biofouling where fluid shear rates are quite high.

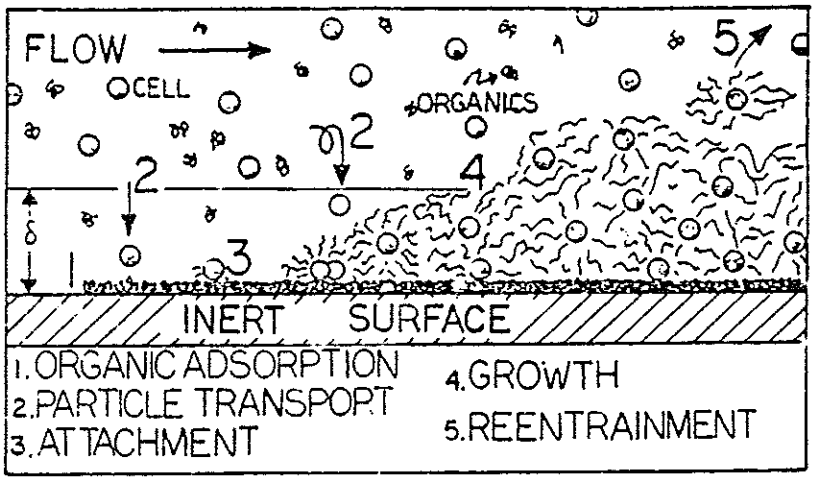

Fig. 2. Summary diagram of hypothesized biofouling processes.

4. Growth of attached microorganisms--Biofilm growth has been described by a wide variety of rate expressions whose rate constants are functions of pH, temperature, limiting nutrient concentration and type, terminal electron acceptor and organism concentration. Postulated rate expressions for nutrient depletion by fixed biofilms are numerous [22-27] but agree that nutrient depletion rates are first order in biofilm mass and that diffusion rates in the biofilm can often control the overall nutrient removal rate.

5. Detachment of attached biofilm--At any point in a biofilm's development, portions of biofilm peel away from the inert surface and are reentrained in the fluid flow. Detachment is a continuous process of biofilm removal and is highly dependent on hydrodynamic conditions [26]. Sloughing, on the other hand, appears to be a random, massive removal of biofilm attributed to oxygen/nutrient depletion deep within biofilms.

In summary, biofouling is the net result of several rate processes occurring simultaneously. However, at specific times in the overall biofilm development, certain processes may contribute more significantly than others.

3. EXPERIMENTAL SECTION

3.1 Research Objectives

Objectives of the research on initial biofilm formation kinetics are as follows:

1. Develop a biofilm detection method(s) sensitive to early stages of biofilm formation,

2. Develop a kinetic expression for initial biofilm accumulation as a function of microbial activity and hydrodynamic parameters,

3. Elucidate those processes which contribute significantly to initial biofilm formation.

3.2 Experimental Protocol

Primary biofilm formation rates are considered dependent upon two factors:

1. The frequency of microorganism contact with the surface

2. The overall growth activity of the suspended microorganisms.

Frequency of microbial contact with an inert surface is assumed directly dependent upon the concentration of suspended organisms and the degree of turbulent intensity; measured, respectively, as the suspended biomass concentration (X) and Reynolds number (Re). Microbial activity is characterized by the dispersed biomass growth rate (μ).

3.3 Reactor System

A tubular biofouling reactor system, illustrated in Fig. 3, was used in this study. The reactor system contained the following components:

1. nutrient feed system

2. two tubular recycle loops

3. biofouling tubular reactor units

4. three-liter plexiglass mixing vessel

Recycle loops were constructed of 1.27 cm I.D. Schedule 80 poly (vinyl chloride) pipe. Flow through the recycle circuit was generated by a rotary helical screw pump; flow rates were set with globe valves and monitored using two cumulative-flow water meters.

The reactor was operated as a C.S.T.R. with an internal recycle circuit; dispersed biomass being generated within the mixing vessel and recycle circuit. This system maintains desired reactor biomass and nutrient concentration and biomass growth rate constant.

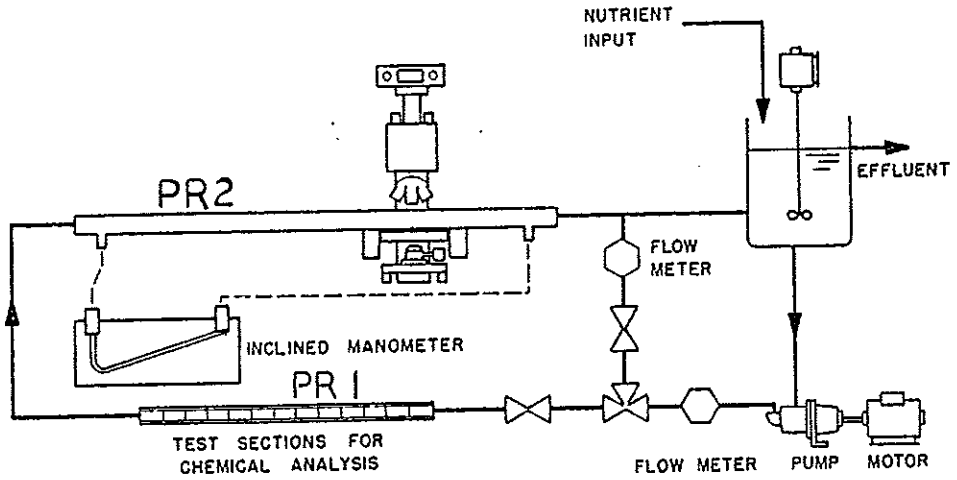

Fig. 3. Experimental system for observing primary film formation.

Two types of tubular fouling units were used in the reactor system to monitor biofouling progression. PR-1 consisted of two parts: (1) fifteen 1.27 cm I.D. x 5.13 cm L cylindrical Pyrex glass test sections within, (2) a 1.63 cm I.D. x 79.6 cm L stainless steel outer tube. Glass sections were periodically withdrawn throughout an experiment to chemically determine biofilm accumulation. For sampling, PR-1 was isolated from the recycle flow by means of a bypass line. The PR-1 unit was then removed from the recycle circuit via two quick-disconnect unions. An exposed test section was removed by inserting a clean replacement section. The unit was then reinserted into the recycle loop and flow reinitiated. Total sampling time was less than two minutes.

Reactor PR-2 was a 1.27 cm I.D. x 91.4 cm L Pyrex glass cylindrical tube equipped with two pressure taps, 2.50 cm from each end. Pressure drop across the reactor was measured with an inclined mercury manometer (range 15.2 cm Hg). Biofilm development on the inner surface of reactor PR-2 was also monitored microscopically.

Nutrient feed system. Design of the nutrient feed system is depicted in Fig. 4. A 1:1 ratio of glucose (J. T. Baker Chemical Co.) and trypticase soy broth (TSB)(Becton, Dickinson and Company, Cockeysville, MS) was used as nutrient. An inlet nutrient concentration of 200 mg/1, for example, was 100 mg/1 glucose and 100 mg/1 TSB.

Separate stock solutions of glucose and TSB were prepared with deionized water. This technique minimized the amount of stock solutions, their frequency of preparation, and chances of contamination. Stock TSB was autoclaved at 20 psi and 121°F for thirty minutes to sterilize the solution. Autoclaving glucose solutions is considered by many to produce microbial toxins. Therefore, glucose was not autoclaved; glucose stock solution concentrations were too high and other essential nutrient (N,P,Fe, etc.) concentrations too low to allow microbial growth.

Nutrients were pumped separately into the mixing vessel with a multi-channel peristaltic pump. Dilution water was pumped through an activated carbon column to the mixing vessel with a second peristaltic pump. Nutrients and dilution water were dripped into the reactor fluid to avoid back contamination of feed lines.

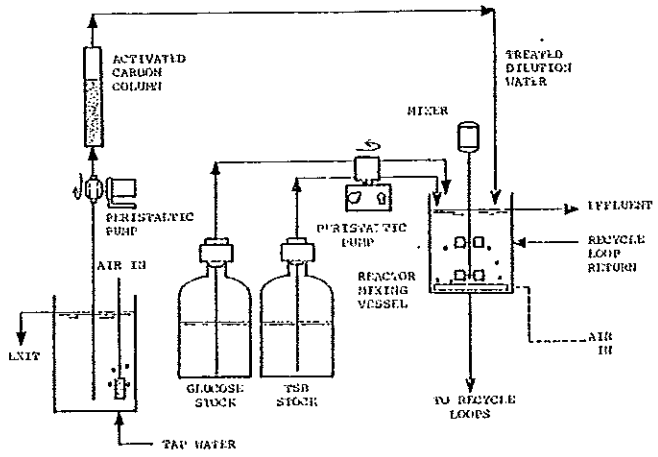

Fig. 4. Nutrient feed system schematic

Microbial inoculum preparation. A standard inoculum was prepared in order to minimize the effects of population variations between experiments. Twenty liters of mixed liquor from the activated sludge basin of a domestic wastewater treatment plant (Bellaire, Texas) was settled and the sludge concentrate mixed with glycerol to 25% glycerol. Ten milliliters of the above suspension were transferred to glass ampules where they were "quick frozen" in liquid nitrogen, then stored at -20°C. Growth rate tests of the standard inocula were periodically made by inoculating 250 milliliters of TSB solution (12 g/l) with an ampule and observing growth indirectly via light transmittance. Results are presented in Table 1 and indicate no significant changes in growth rates over a year period for the first group of inoculum. Growth rates of 25% and 12% of those for inoculum I were observed respectively for the second and third inoculum series. Differences are attributed primarily to a change in procedure, although population differences could certainly affect viability.

Table 1. Batch growth rates of standard inocula (in 250 mg trypticase soy broth; initial concentration = 12 g/l TSB)

	Average Growth Rate (hr^{-1})	Generation Time (min)
INOCULUM I:		
November 24, 1976	1.38 ± 0.09 (6)*	43.5
December 7, 1976	1.52 ± 0.16 (2)	39.5
January 21, 1977	1.43 ± 0.03 (2)	42.0
November 10, 1977	1.22 ± 0.08 (2)	49.0
INOCULUM II:		
December 30, 1977	0.31 ± 0.03 (3)	193.5
INOCULUM III:		
January 31, 1979	0.20 ± 0.04 (2)	306.0

* ( ) indicate the number of replicate tests

3.4 Analytical Methods

Chemical oxygen demand (COD) was used to indirectly characterize the amount of organic carbon in the nutrient feed, reactor effluent, and attached biofilm. A modified procedure of the standard COD [28] was used to detect the anticipated low levels of carbon present.

Total suspended biomass in the reactor fluid was determined by a membrane filtration-gravimetric procedure. Periodically, two 100 ml samples of reactor fluid were withdrawn and filtered through two tared 0.45 μm Nuclepore filters. Filters were dried at 60°F for a three-hour period and stored in a dessicator until weighed. Biomass concentration was calculated as the ratio of the net filter weight increase to the volume filtered.

Total polysaccharide concentration in the bulk fluid and attached biofilm was determined colorimetrically using the phenol-sulfuric acid method as out-

lined by Dubois et al.,[29]. Simple sugars, oligosaccharides, and polysaccharides with free reducing groups render an orange-yellow color proportional to concentration when treated with phenol and concentrated sulfuric acid. The polysaccharide determination was calibrated with aqueous glucose solutions.

Total protein concentrations in the bulk fluid and attached biofilm were determined by either ultra-violet absorbance at 280 nm [30] or by the method of Lowry et al., [31]. Direct absorbances at 280 nm were corrected for the amount of nucleic acids present. Both protein methods were calibrated with casein dissolved in 3.0% wt aqueous NaOH solution and gave similar results.

Total nucleic acid (NA) content of reactor fluid and attached biofilm was determined using absorbance at 260 nm after a hot NaOH hydrolysis as detailed by Echlin and DeLamater [32]. No calibration between absorbance and concentrations was determined; results are reported as absorbance at 260 nm.

3.5 Biofilm Detection Methods

During the growth and plateau phases, biofilm accumulation can be monitored by the several methods listed in Table 2. Analytical details of these methods are given elsewhere [33].

The direct and indirect biofilm detection methods are excellent measures of biofouling during the latter stages of biofilm development as indicated by other investigators [1,27,33,34].

However, lack of both sensitivity and precision restricts use of these methods to the latter two stages of biofilm accumulation [34]. Table 3 lists the sensitivity and precisions for the direct detection methods.

Table 2. Measurement of biofouling

A.	Direct Measurement of Biofilm Quantity	
	Thickness	
	Mass	
B.	Indirect Measurement: Measurement of Biofilm Effects	
	Frictional Resistance	
	Heat Transfer Resistance	
C.	Measurement of Specific Biofilm Constituent	
	Polysaccharide	Organic Carbon
	Chemical Oxygen Demand	Protein
D.	Measurement of Biofilm Microbial Activity	
	Viable Cell Count	Lipopolysaccharide
	ATP	Nucleic Acid Content
E.	Microscopic Surveillance	

Table 3. Limits of direct biofilm detection methods

Methods	Sensitivity		Precision		Reference
Biofilm Thickness	Thickness (μm)	Attached Carbon* (μgCOD/cm^2)	Thickness (μm)	Attached Carbon* (μgCOD/cm^2)	
	9	25.6	± 9	±25.6	[27]
	10	28.5	±10	±28.5	[25]
	10	28.5	± 9	±25.6	[26]
Biofilm Mass	Mass (mg/cm^2)	Attached Carbon* (μgCOD/cm^2)	Mass (mg/cm^2)	Attached Carbon* (μgCOD/cm^2)	
	0.11	0.125	.01	.285	[27]

*Calculated from thickness values assuming biofilm density = 25 mg/cm^3 and 1.14 mgCOD/mg biomass. Reference: Trulear [26] and Bryers [17].

Evidence indicates that the minimum biofilm detection limit of frictional resistance methods is set by the hydrodynamics of the system; specifically, the viscous sublayer thickness. Experimental observation shows no frictional resistance increases until biofilm thicknesses exceed the viscous sublayer [1,26, 27]. Reiterating, initial biofilm formation ceases, by convention, when the frictional resistance increases. Therefore, biofilm surveillance based upon analysis of either a biofilm or a viable cell constituent was necessary. Examples of these methods are provided in Table 2.

Attached biofilm: sampling and chemical analysis. Biofilm amount attached to glass test sections of Reactor PR-1 was determined by several chemical methods. To optimize the amount of biofilm material recovered per test section, the following standard sample preparation procedure was employed:

1. Two glass sections were removed at prescribed intervals and rinsed with distilled water to remove any non-attached biomass.

2. Each glass section was then submerged in 0.025 liters of double distilled water in a pre-cleaned 2.25 cm I.D. x 20.0 cm L glass culture tube.

3. The contents of each culture tube were then subjected to a one-minute ultrasonic treatment to disrupt and disperse all attached material uniformly throughout the solution.

4. Protein, nucleic acid, and polysaccharide content of the dispersed attached biofilm was determined. Three milliliters of sample fluid were required for these analyses.

5. Five milliliters of concentrated sulfuric acid containing 0.54% wt Ag_2SO_4 was then added to the remaining 22.0 ml and each tube sealed.

6. Contents of each culture tube including both the acidic solution and glass section were transferred to distillation flasks for a modified COD analysis to determine the amount of attached chemically oxidizable material.

Attached biofilm: photomicrographic surveillance. The number of attached fibril colonies per area of reactor PR-2 was recorded using a Bausch and Lomb compound microscope with a Pentax SLR 35 mm camera adaptation. Maximum magnification of the camera modification was 500 x (10x eyepiece · 10x ocular · 2x zoom factor · 2.5x camera factor). Resolving power was 2.0 μm (λ = 0.5 μm, numerical aperture = 0.25).

Due to the similarity in refractive index of attached biofilms and the bulk fluid, some artificial means of enhancing their contrast for photographs was desired. Chemical cytological staining was disregarded due to possible detrimental effects upon adhering organisms. Use of a high contrast film (Kodak SO-115 Technical Pan Film) coupled with an optical staining technique proved effective. Optical staining consisted of simultaneous application of two filtered light sources. Direct light of the microscope was filtered with a Kodak Wratten No. 25 red filter while a second light, filtered through a Kodak Wratten No. 45 blue filter, was applied at an oblique angle.

The oblique blue light was reflected from any attached biofilm but was not as discernible to the red-light sensitive film as the red-filtered primary source. Results were an over-exposed (light, pale) background with dark under-exposed attached biofilm fibers.

The number of fibers attached were visually counted from resultant photographs. The area in a photograph frame was 0.0063 cm^2 as determined from a photograph of a stage micrometer.

5. RESULTS

Procedure. The above system was used to evaluate the rates of initial biofouling as a function of the three parameters; dispersed biomass concentration (X), Reynolds Number (Re), and dispersed organism growth rate (μ).

Portions of the reactor system, the mixing vessel and Loop One, were operated as a continuous cell propagator until dispersed biomass and effluent nutrient concentrations reached a steady-state. Biofouling tubular reactors, situated in Loop Two, were then exposed to fluid flow of known velocity. This was considered zero time. Experiments were terminated at the onset of any frictional resistance increase.

Experiments are arranged in three groups according to which one of the three parameters was being considered. Detailed experimental conditions are provided in Table 4.

Results. Figures 5, 6, and 7 exemplify biofilm accumulation results, as μg COD/cm^2, from typical experiments selected from the biomass concentration, Reynolds number, and growth rate experiment group, respectively.

Figure 5 illustrates a decreasing initial biofilm induction rate with descreasing dispersed biomass concentration, at constant Re (17,200) and μ (0.277 h^{-1}).

The Reynolds number experiments were conducted at constant biomass concen-

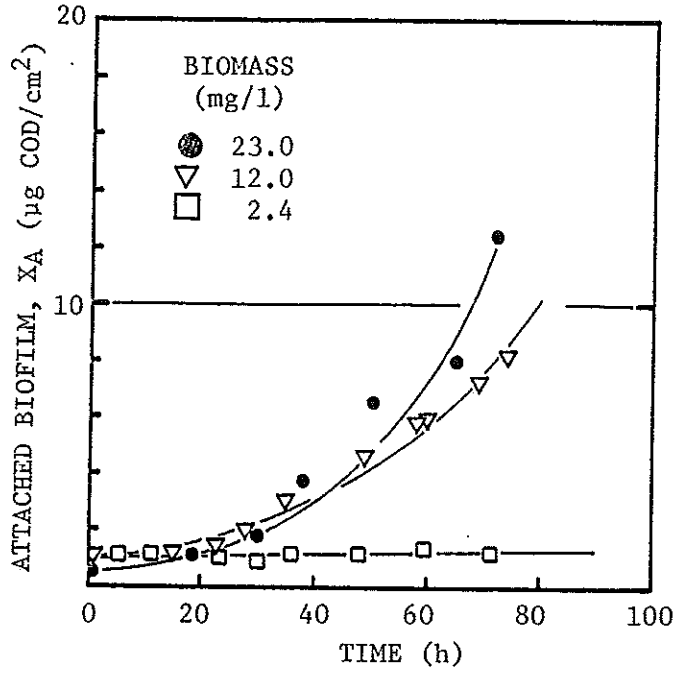

Fig. 5. Initial biofilm formation at various dispersed biomass concentrations. Re = 17,200 and μ = 0.277 h^{-1}. Equation 13 shown as solid line.

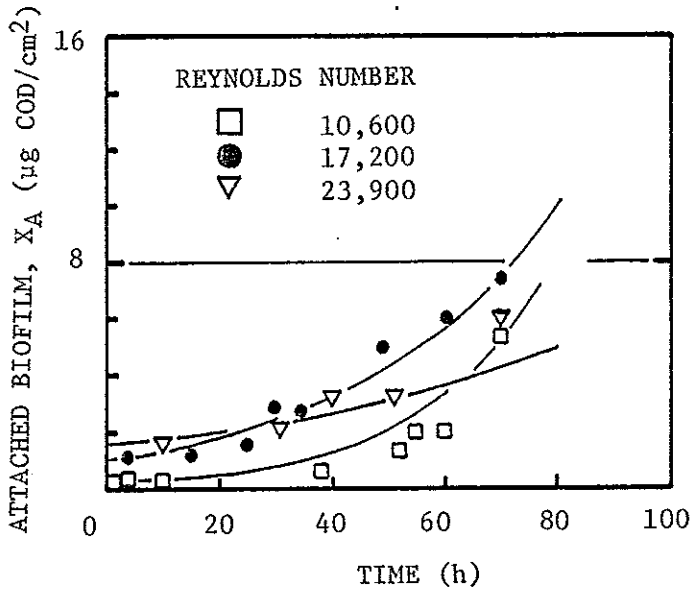

Fig. 6. Initial biofilm formation at various Reynolds numbers. X = 12.0 mg TSS/1 and μ = .277 h^{-1}. Equation 13 shown as solid line.

Table 4. Experimental Conditions.

EXPERIMENT Number	Group	X (mg TSS/1)	μ (h^{-1})	Re x 10^{-3}
1	Biomass	4.4	0.277	17.2
2		12.0	0.277	17.2
3		2.8	0.277	17.2
4		13.0	0.277	17.2
5		23.0	0.277	17.2
6		4.0	0.277	17.2
7		10.1	0.277	17.2
8		2.5	0.277	17.2
9	Reynolds	12.0	0.277	17.2
10	Number	12.0	0.277	10.6
11		12.0	0.277	19.3
12		12.0	0.277	23.9
13		12.0	0.277	28.8
14	Dispersed	18.0	.983	17.2
15	Growth Rate	18.0	.277	17.2
16		18.0	.163	17.2
17		18.0	.125	17.2
18		18.0	.125	17.2

trations and dispersed growth rate of 12 mg TSS/1 and 0.277 h^{-1}, respectively. Figure 6 illustrates a decrease in overall initial biofilm development with increasing Reynolds number.

Increasing dispersed biomass growth rate markedly increases the rate of initial biofilm formation as exemplified in Fig. 7. Dispersed biomass and Reynolds number were constant at 18 mg TSS/1 and 17200, respectively.

Biofilm development was also monitored indirectly using a microscopic observation (attached fiber number/area), total polysaccharide attached, total nucleic acid, and total attached protein. Examples of these results for Experiment 14 are illustrated in Figs. 8-10. Notice that indirect measures of biofilm quantity (e.g., COD, fiber count, total polysaccharide) increased non-linearly while measures of biofilm activity (e.g., nucleic acids, proteins) increased linearly.

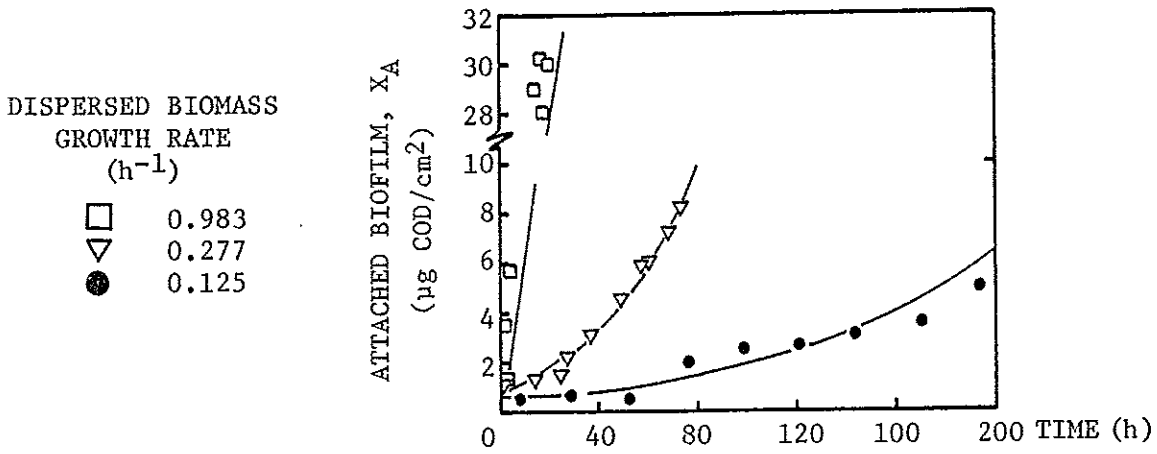

Fig. 7. Initial biofilm formation at various dispersed biomass growth rates. Re = 17,200 and X = 18.0 mgTSS/1 Equation 13 shown as solid line.

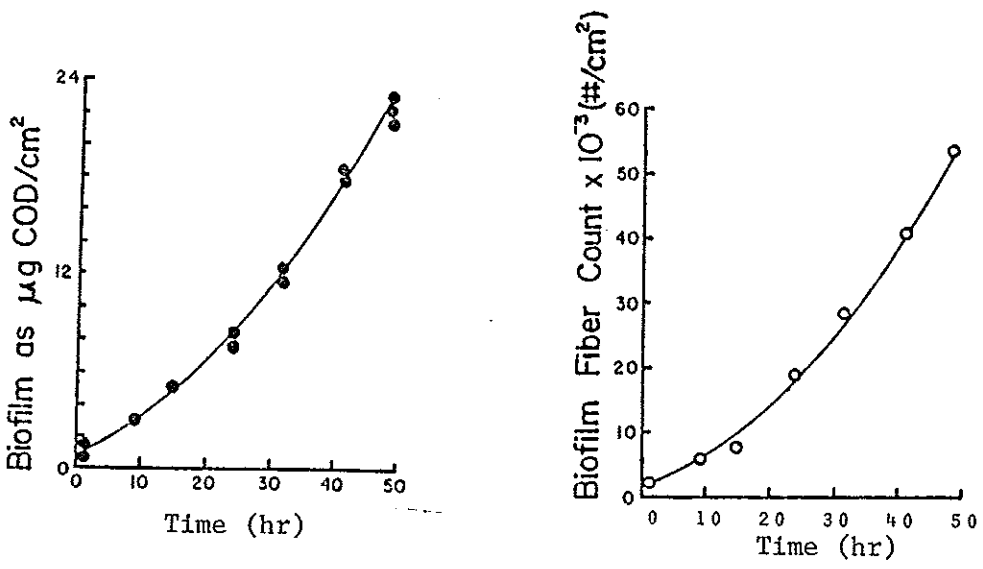

Fig. 8. Biofilm development as determined by biofilm fiber count and chemical oxygen demand per unit area

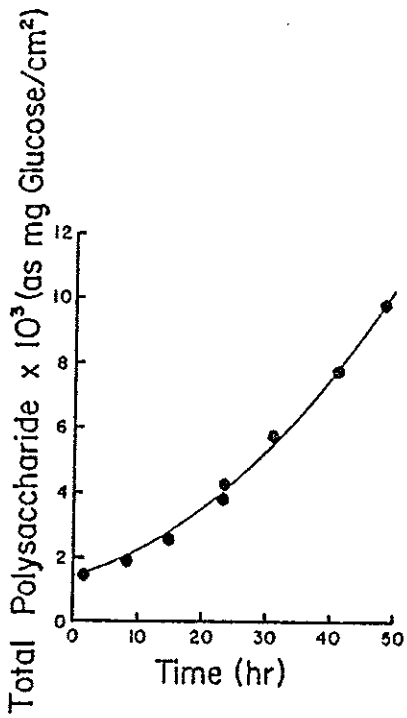

Fig. 9. Increase in biofilm polysaccharide

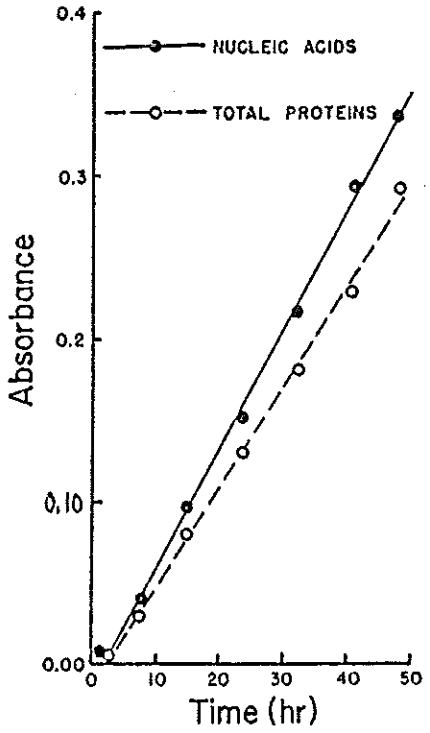

Fig. 10. Biofilm development as determined by total attached nucleic acids and total attached proteins.

Mathematical interpretations. Kinetics of the initial biofilm accumulation rate were determined from material balances on the reactor system. Material balances on dispersed biomass and limiting nutrient can be written as follows:

$$\left[\begin{array}{c}\text{Dispersed}\\ \text{Biomass}\\ \text{Accumulation}\end{array}\right] = \left[\begin{array}{c}\text{Net Biomass}\\ \text{Inflow}\\ \text{Rate}\end{array}\right] + \left[\begin{array}{c}\text{Dispersed}\\ \text{Biological}\\ \text{Growth}\\ \text{Rate}\end{array}\right] + \left[\begin{array}{c}\text{Biofilm}\\ \text{Reentrainment}\\ \text{Rate}\end{array}\right]$$

$$\frac{dX}{dt} = \frac{F}{V}(X_i - X) + \mu \cdot X + k_s f_3(X_A) \quad (1)$$

where X = dispersed biomass concentration (ML^{-3})

F = volumetric flow rate (L^3t^{-1})

V = reactor system volume (L^3)

μ = dispersed biomass growth rate (t^{-1})

k_s = shear reentrainment rate (t^{-1})

$f_3(X_A)$ = shear reentrainment, a function of attached biofilm (M/L^2)

X_A = attached biofilm ($M\text{-}L^2$)

and

$$\left[\begin{array}{c}\text{Limiting}\\ \text{Nutrient}\\ \text{Accumulation}\end{array}\right] = \left[\begin{array}{c}\text{Net Nutrient}\\ \text{Inflow}\\ \text{Rate}\end{array}\right] - \left[\begin{array}{c}\text{Dispersed}\\ \text{Organism}\\ \text{Nutrient}\\ \text{Depletion Rate}\end{array}\right] - \left[\begin{array}{c}\text{Attached}\\ \text{Organism}\\ \text{Nutrient}\\ \text{Depletion}\\ \text{Rate}\end{array}\right]$$

$$\frac{dS}{dt} = \frac{F}{V}(S_i - S) - \mu X/Y - \frac{k_g}{Y} f_2(X_A) \quad (2)$$

where S = nutrient concentration $(M\text{-}L^3)$

Y = biomass yield coefficient (-)

k_g = attached biofilm growth rate (t^{-1})

$f_2(X_A)$ = attached biofilm growth, a function of attached biofilm $(M\text{-}L^{-2})$

Equations 1 and 2 require an additional equation describing biofilm accumulation, which is written as follows:

$$\left[\begin{array}{c}\text{Initial Biofilm}\\ \text{Accumulation}\\ \text{Rate}\end{array}\right] = \left[\begin{array}{c}\text{Microorganism}\\ \text{Deposition and}\\ \text{Attachment Rate}\end{array}\right] + \left[\begin{array}{c}\text{Attached}\\ \text{Biofilm}\\ \text{Growth Rate}\end{array}\right] - \left[\begin{array}{c}\text{Attached}\\ \text{Biofilm}\\ \text{Rate}\end{array}\right]$$

$$\frac{dX_A}{dt} = k_d f_1(X_A) + k_g f_2(X_A) - k_s f_3(X_A) \quad (3)$$

where k_d = biomass deposition rate constant (L^{-1})

$f_1(X_A)$ = biomass deposition, a function of attached biofilm $(M\text{-}L^{-2})$

Equations 1-3 can be simplified with the following assumptions:

1. Effluent biomass and nutrient concentration are at a steady state
2. Inlet biomass concentration is zero
3. Nutrient depletion by attached biofilms is negligible compared to that of the dispersed organisms.

All assumptions were experimentally verified [17]. Equations 1-3 reduce to the following:

$$F/V = \mu \quad (4)$$

$$Y(S_i - S) = X \quad (5)$$

$$dX_A/dt = k\, f_4(X_A) \quad (6)$$

where k = initial biofilm accumulation rate constant (t^{-1})

$f_4(X_A)$ = overall accumulation rate, a function of attached biofilm amount $(M\text{-}L^{-2})$

Equations 4 and 5 are the familiar expressions for the steady-state chemostat.

Equation 6 describes the overall rate of initial biofilm accumulation. The non-linear increase of biofilm amount with time suggests a first order rate expression of the form:

$$dX_A/dt = k\ X_A \tag{7}$$

The numerical value of the rate constant, k, was determined from statistical regression of X_A versus time data according to the integrated form of Equation 7. These values of k are illustrated for each experiment group in Figures 11 - 13.

The overall rate constant, k, is considered a function of the three chosen system parameters, i.e.,

$$k = k_1\ X^a Re^b \mu^c \tag{8}$$

where k = initial biofilm accumulation rate (t^{-1})

k_1 = specific biofilm accumulation rate constant (L^3-M^{-1})

a,b,c = rate "orders" of selected parameters

Figure 11 presents a linear dependency of k on the dispersed biomass concentration, X. A linear statistical correlation of k to X yields the following:

$$k = k^*\ X^{1.0} \tag{9}$$

where $k^* = k_1 Re^b \mu^c = 0.004$ l - $mgTss^{-1}$ - hr^{-1}

An increase in Reynolds number, Re, results in a linear decrease in initial biofilm accumulation rate, k, as illustrated in Figure 12. Correlation of k to Re yields

$$k = k^{\#}(Re)^{-1.0} \tag{10}$$

where $k^{\#} = k_1 X^{1.0} \mu^c = 1.45 \times 10^{+3}\ h^{-1}$

Figure 13 indicates that the initial biofouling accumulation rate, k, is also a linear function of the dispersed organism growth rate, μ. Statistical regression yields a linear expression of the form:

$$k = k^{**}\mu \tag{11}$$

where $k^{**} = k_1 X^{1.0} Re^{-1.0} = 0.069$

Once the orders a,b,c are known, the specific rate constant, k_1 can be calculated from any known set of experimental conditions.

Using Equations 9 - 11, Equation 7 can be rewritten as follows:

$$dX_A/dt = k_1(X \cdot \mu/Re)\ X_A \tag{12}$$

where $k_1 = 125.0 \pm 25.0$ l-$mgTSS^{-1}$

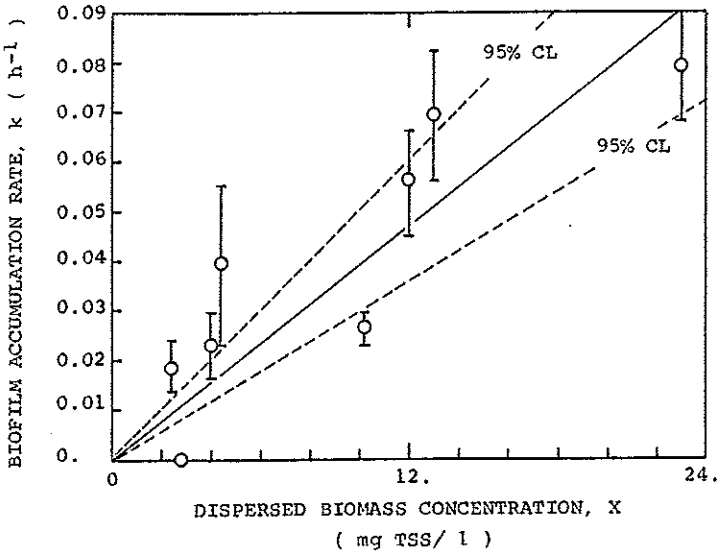

Fig. 11. Biofilm accumulation rate as a function of dispersion biomass concentration. Re = 17,200 and $\mu = 0.277\ h^{-1}$

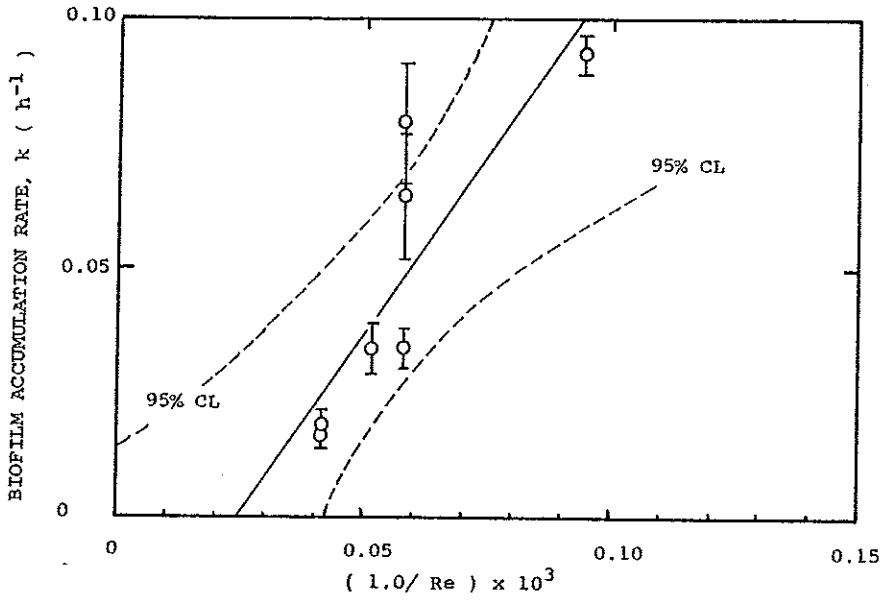

Fig. 12. Biofilm accumulation rate as a function of Re. X = 12. mgTSS/l and $\mu = 0.277\ h^{-1}$

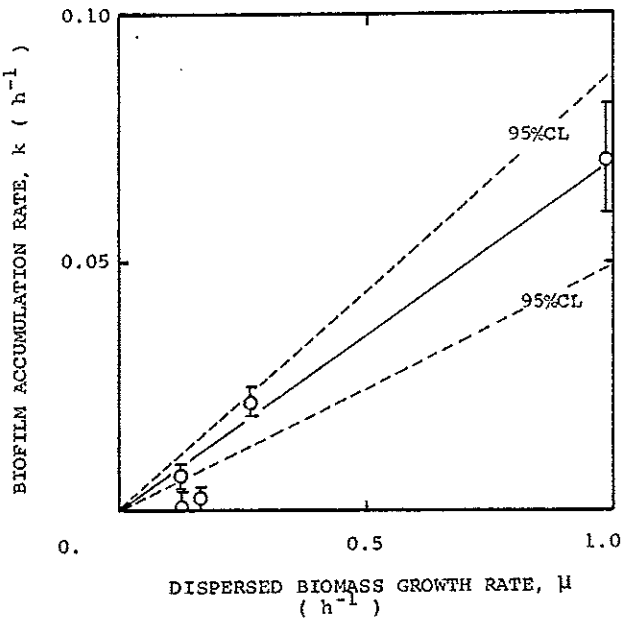

Fig. 13. Biofilm accumulation rate as a function of dispersed biomass growth rate. Re = 17,200 and X = 18 mg TSS/1

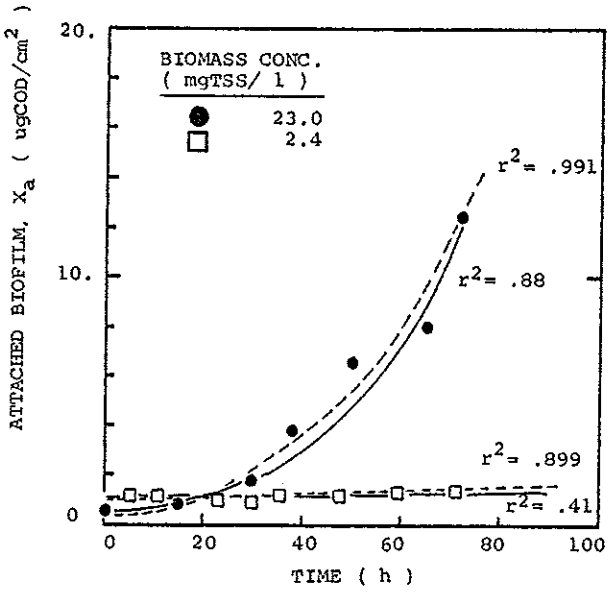

Fig. 14. Comparison of exponential regression (solid line) to polynomial regression (dashed line) for experiments at two different biomass concentrations. Re = 17,200 and μ = .277 h^{-1} (r^2 = correlation coefficient)

The integrated form of Equation 12,

$$X_A = X_{A_o} \exp(k_1 X \mu t / Re) \tag{13}$$

is evaluated for selected experiments and plotted in Figures 5-7 for comparison to actual data.

In certain experiments, k values with poor correlation coefficients (r^2 values) and large confidence limits were obtained. Biofilm accumulation in these experiments was linear rather than exponential in appearance and correlation to the first order rate expression was predictably poor. A Taylor series expansion of the exponential term in Equation 13 yields

$$X_A = C_1 + C_2 t + C_3 t^2 + C_4 t^3 + \ldots \tag{14}$$

where C_{1-4} = constants of the multiple regression

Statistical correlations of X_A versus time data, using Equation 14 provide an excellent correlation of all experiments. Those biofilm accumulation experiments with linear responses also correlated well with the nonlinear second and third ordered terms vanishing. A comparison of both correlations to experimental data is shown in Figure 14. A shift in the relative magnitude of the fundamental rate processes contributing to overall accumulation is suggested.

It must be noted that Equations 12 and 13 are empirical rate expressions which describe the overall rate of accumulation of biofilm within the initial stages of development. The effect of X, Re, and μ on the rate are those observed for the overall accumulation within this reactor system. The above analysis does provide a simple empirical expression for biofilm accumulation in the early stages of formation in turbulent flow for the range of variables cited. An in-depth consideration of the more fundamental rate processes that contribute to initial biofouling is presented by Bryers [17].

6. SUMMARY

The influence of three parameters - dispersed biomass concentration (X), Reynolds number (Re), and dispersed biomass growth rate (μ) - on initial biofilm formation has been described in this paper. Effects of these chosen parameters on more fundamental processes involved in biofilm accumulation are presented elsewhere [17].

Biofouling experiments were conducted in a CSTR with internal recycle at constant biological activity and turbulent intensity. Results provided the following information:

1. Chemical techniques (COD and total polysaccharide) provided sensitive measures of biofilm accumulation prior to the observation of any fluid frictional resistance changes.

2. Total biofilm accumulation does not increase proportionally with biofilm cellular concentration. For example, attached biofilm (as $\mu gCOD/cm^2$) increases non-linearly with time while total attached nucleic acids increase linearly. Results suggests that the production rate of attached extracellular polysaccharides increases during biofouling.

7. Perrigo, L.D. 1977. Battelle OTEC Biofouling Project. private communication.

8. Fetkovich, J. 1979. private communications.

9. Baier, R.E., E.G. Shafin, and W.A. Zisman. 1968. Adhesion: Mechanisms that Assist or Impede It. Science. 162(2):1360.

10. Baier, R.E. 1972. Influence of the Initial Surface Condition of Materials on Bioadhesion. Proc. 3rd Int'1. Cong. on Marine Corr. and Biofouling, Oct 2-6,

11. Baier, E.E. (ed.) 1973. Applied Chemistry at Protein Interfaces. #145. American Chemical Society, p. 1.

12. Loeb, G. and R. Neihof. 1972. Molecular Fouling of Surfaces in Seawater. Proc. 3rd Int'1. Cong. on Marine Corr. and Biofouling, Oct. 2-6, Gaithersburg, MD.

13. Loeb, G. and R. Neihof. 1973. Marine Conditioning Films. Adv. Chem. Series #145. American Chemical Society. p. 319.

14. Dexter, S.C., J.D. Sullivan, J. Williams, S.W. Watson. 1975. Influence of Substrate Wettability on the Attachment of Marine Bacteria to Various Surfaces. Applied Microbiol. 30(2):298-308.

15. Friedlander, S.K. and H.F. Johnstone. 1957. Deposition of Suspended Particles from Turbulent Gas Streams. I. and E.C. 49(2):1151-1156.

16. Beal, S.K. 1970. Deposition of Particles in Turbulent Flow on Channel or Pipe Walls. Nucl. Sci. and Engr. 40:1-11.

17. Bryers, J.D. 1979. Rates of Initial Biofilm Formation within a Turbulent Flow System. Ph.D. Dissertation. Rice University.

18. Corpe, W.A. 1970. Attachment of Marine Bacteria to Solid Surfaces. In: Adhesion in Biological Systems. R.S. Manly, ed. Academic Press, New York.

19. Corpe, W.A. 1972. Microfouling: The Role of Primary Film Forming Bacteria. Proc. 3rd Int. Congr. on Marine Corrosion and Fouling, Oct. 2-6, Gaithersburg, MD.

20. Marshall, K.C. 1977. Mechanism of Adhesion of Marine Bacteria to Surfaces. Proc. 3rd Int'1. Cong. on Mar. Corr. and Biofouling, Oct. 2-6, Gaithersburg, MD.

21. Fletcher, M. and G.D. Floodgate. 1973. An Electron Microscopic Demonstration of an Acidic Polysaccharide Involved in the Adhesion of a Marine Bacterium to Solid Surfaces. J. Gen. Microbiol. 74:325-334.

22. Atkinson, B. and M.E. Abdel Rahman Ali. 1976. Wetted Area, Slime Thickness, and Liquid Phase Mass Transfer in Packed Bed Biological Film Reactors. Trans. Inst. Chem. Engr. 54:239-250.

23. Harremoes, P. 1977. Half-order Reactions in Biofilm Kinetics. Vatten. 2: 122-143.

24. Kornegay, B.H. 1967. Characteristics and Kinetics of Biological Fixed Film Reactors. Ph.D. Disseration, Clemson University, Clemson, S.C.

3. The rate of initial biofilm accumulation was described mathematically using a first order rate expression. The resultant first order rate constant k was a linear function of X, Re, and μ according to Equation 13:

$$X_A(t) = X_{A_o} \cdot \exp(125.0\ \ 1\text{-}\ mgTSS^{-1}\ X\mu t/Re)$$

4. Overall biofilm accumulation rate increased with increasing dispersed biomass concentration over the range of 2.0 - 27.0 mgTSS/1. Mass transport theory [35] and particle deposition theory [15,16] indicate the particle flux to a surface is directly proportional to the bulk particle concentration.

5. Biofilm accumulation rate increases with increasing dispersed organism growth rate.

6. Mass transport consideration indicates particle flux from the bulk fluid to the wall increases with increasing Reynolds number, Re. Experimental results indicate a decrease in initial biofilm accumulation with increasing Re, suggesting that particle flux from the bulk fluid is but one of many rate processes contributing to overall biofilm accumulation.

ACKNOWLEDGMENTS

This entire work was conducted at the Environmental Science and Engineering Department, Rice University - Houston, Texas, U.S.A. The authors acknowledge partial support of this project by the following funding agencies: National Science Foundation (ENG 77-26934), Electric Power Research Institute, EPRI, (RP 902-1), Amoco Research Fellowship, and a Sigma Xi Grant-in-Aid of Research. The typing and artistic quality of this manuscript are direct results of both Mlle. Linda Graetz and Ms. Maurine Lee.

REFERENCES

1. Norrman, G. 1976. Biofilm Control in Circular Tubes with Chlorine. M.S. Thesis, Rice University.

2. Characklis, W.G. 1967. Oxygen Transfer through Biological Slimes. M.S. Thesis, University of Toledo.

3. Characklis, W.G. 1970. Effect of Hypochlorite on Microbial Slimes. Ph.D. Dissertation, Johns Hopkins Univ.

4. Characklis, W.G. 1973a,b. Attached Microbial Growths. Water Research. 7: Part a:113-1127, Part b:1249-1258.

5. Hartman, L. 1967. Influence of Turbulence on the Activity of Bacterial Slimes. J. Wat. Pol. Cont. Fed. 39(6):958-964.

6. Heukelekian, H. and E.S. Crosby. 1956. Slime Formation in Polluted Waters. Sew. Indus. Wastes J. 28(2):206.

25. LaMotta, E.J. 1974. Evaluation of Diffusional Resistances in Substrate Utilization by Biological Films. Ph.D. Dissertation, Univ. of North Carolina at Chapel Hill.

26. Trulear, M. and W.G. Characklis. 1979. Dynamics of Biofilm Processes. Proc. 34th Ann. Ind. Wastewater Trtmt. Conf., Purdue University, Lafayette, Indiana.

27. Zelver, N. 1979. Biofilm Development and Associated Energy Losses in Water Conduits. M.S. Thesis, Rice University, Houston, Tx.

28. -- 1975. Standard Methods for the Examination of Water and Wastewater. Am. Public Health Assoc. 14th ed.

29. Dubois, M., K.A. Gilles, J.K. Hamilton, P.A. Rebersand, F. Smith. 1956. A Colorimetric Method for Determination of Sugars and Related Substances. Anal. Chem. 28(3):350-356.

30. Lehninger, A.L. 1975. Biochemistry. 2nd ed. Worth Publishers, Inc. New York.

31. Lowry, O.H., N.J. Rosebrough, A.L. Farr, R.J. Randall. 1951. A Colorimetric Analysis of Proteins. J. Biol. Chem. 193:265-275.

32. Echlin, P. and E.D. DeLameter. 1962. A Cytological and Chemical Analysis of the Bacteria Nucleus. Part II. Exp. Cell Res. 26:229-252.

33. Characklis, W.G. 1979. Biofilm Development and Destruction. Final Report. Electric Power Research Inst. RP902-1, Palo Alto, CA.

34. Characklis, W.G. 1979. Measurement of Biofilm Development. Proc. Condenser Biofouling Control Symposium. Atlanta, Ga. Electric Power Research Inst.

35. Bird, R.B., W.E. Stewart, and E.N. Lightfoot. 1960. Transport Phenomena. J. Wiley and Sons, Inc. New York.